



OPEN Punicalagin relieves hepatic injury by antioxidation and enhancement of autophagy in diet-induced nonalcoholic steatohepatitis

Li Ma, Hanbing Sun, Nian Xiang & Qiushi Xu

Hepatic injury induced by many factors play a central role in the pathogenesis of liver diseases. Punicalagin (PUN) is a major antioxidant polyphenolic compound extracted from pomegranates. The aim of this study was to investigate the potential role of PUN on liver injury induced by nonalcoholic steatohepatitis (NASH). Therefore, the effects and mechanistic action of PUN on NASH mouse model induced by choline-deficient, L-amino acid- defined, high-fat (CDAH) diet were investigated in vivo. Wild-type or nuclear erythroid 2-related factor 2 (Nrf2) KO mice were fed with CDAH diet to induce NASH and then treated with PUN (100, 300 or 500 mg kg⁻¹ day⁻¹) by gavage for 12 weeks. Blood and liver samples were collected to assess liver function, oxidative stress, inflammation, and autophagy pathological status. The results showed that 300 mg/kg PUN was the optimal concentration for relieving hepatic injury in NASH, characterized by decreased activities of serum alanine transaminase, aspartate aminotransferase, and liver lactate dehydrogenase activity and histopathological structural damage, and showed a hepatoprotective effect against NASH. PUN significantly reduced the level of liver inflammation and Txnip-NLRP3 signaling pathway in NASH mice. PUN reduced oxidative stress by reducing liver malondialdehyde levels and the accumulation of reactive oxygen species (ROS) and increasing liver superoxide dismutase and glutathione peroxidase activity. PUN may also attenuate oxidative stress and induce autophagy through the p62/Nrf2 and AMPK/mTOR/ULK1 pathway. More importantly, we found that these protective effects of PUN were attributed to enhanced antioxidant, anti-inflammatory and autophagy activity, which was mediated by the activation of the Nrf2 pathway using Nrf2 KO mice. In summary, the present results indicate that PUN successfully relieved NASH-induced liver damage by upregulating Nrf2 signaling and autophagy.

Keywords Punicalagin, NASH, Txnip-NLRP3 signaling, Nrf2, Oxidative stress, Autophagy

Nonalcoholic fatty liver disease (NAFLD), which is currently on the rise with obesity prevalence, is the most common chronic liver disease and may develop into nonalcoholic steatohepatitis (NASH)¹. NASH is characterized by oxidative damage, inflammatory cellular infiltration into the liver, and varying degrees of fibrosis, and may lead to occurrence of liver cirrhosis or hepatocellular carcinoma^{2,3}. Therefore, there is an urgency to identify the molecular and cellular mechanisms underlying the development of NASH and related hepatitis.

Nuclear factor E2-related factor 2 (Nrf2) is a cytoprotective regulator known to protect against oxidative stress^{4,5}. Activation of Nrf2 leads to the transcription of a variety of antioxidants and detoxification enzymes, and plays an important role in reducing the damage induced by oxidative stress in cells when challenged by stress^{6,7}. Induction of Nrf2 protects against inflammation and oxidative damage in the pathogenesis of liver injury in vitro and in vivo^{8,9}.

Autophagy is a homeostatic cellular degradation process that can remove damaged organelles or reverse cytoplasmic components through the lysosomal compartment in eukaryotic cells. It is shown that autophagy is widely regarded as a key regulator of cell survival and homeostasis, and a lack of autophagy can promote inflammation, oxidative stress, apoptosis and cause diseases in various tissues^{10,11}. In particular, recent observations indicate that the AMPK/mTOR/ULK1 axis induces autophagy-dependent apoptosis in human bladder cancer cells¹². Therefore, autophagy can reduce apoptotic factors and reduce liver damage by regulating activation of the AMPK/mTOR/ULK1-pathway. Therefore, autophagy can be activated by drug therapy to

College of Animal Science and Veterinary Medicine, Heilongjiang Bayi Agricultural University, Xinfeng Rd. 5, Daqing 163319, China. email: xuqiushi0903@126.com

prevent liver damage caused by NASH¹³. The strategy of activating Nrf2 and resolving autophagy dysfunction seems to be beneficial to the treatment of NASH.

Punicalagin (PUN) is the main biologically active ingredient in pomegranate peel. It has a variety of biological effects and has been proven to have antioxidant, anti-inflammatory, and antiobesity properties¹⁴. The antioxidant activity of PUN has been studied in the liver of patients with type 2 diabetes mellitus¹⁵, and in cardiovascular diseases¹⁶. The existing literature shows that it may be closely related to liver disease^{17,18}. However, the mechanisms of the antioxidant and anti-inflammatory effects of PUN in NASH have rarely been studied. Therefore, the purpose of this study was to clarify the effect of PUN on NASH and identify the underlying mechanisms, to optimize treatment strategies.

Results

PUN alleviated liver injury in diet-induced NASH

Compared with the control group, treatment with vehicle and PUN (500 mg/kg) had no significant effect on serum activities of alanine aminotransferase (ALT) and aspartate aminotransferase (AST) or hydroxyproline concentrations in liver samples (Fig. 1A–C). Furthermore, compared with the NASH group, the decline in serum activities of ALT and AST was most significant in mice treated with 300 mg/kg PUN (Fig. 1D, E). Administration of PUN at various concentrations prevented pathological changes and inflammation in hepatocytes (Fig. 1F, G). Masson's trichrome staining, which is used to detect liver fibrosis, revealed the same results as hematoxylin and eosin staining (Fig. 1F, G). However, treatment with 300 mg/kg PUN showed mild degeneration, and hepatocyte nuclei and hepatic cords maintained their normal morphology (Fig. 1F, G). Thus, these results indicated that PUN protected against the hepatic injury in diet-induced NASH.

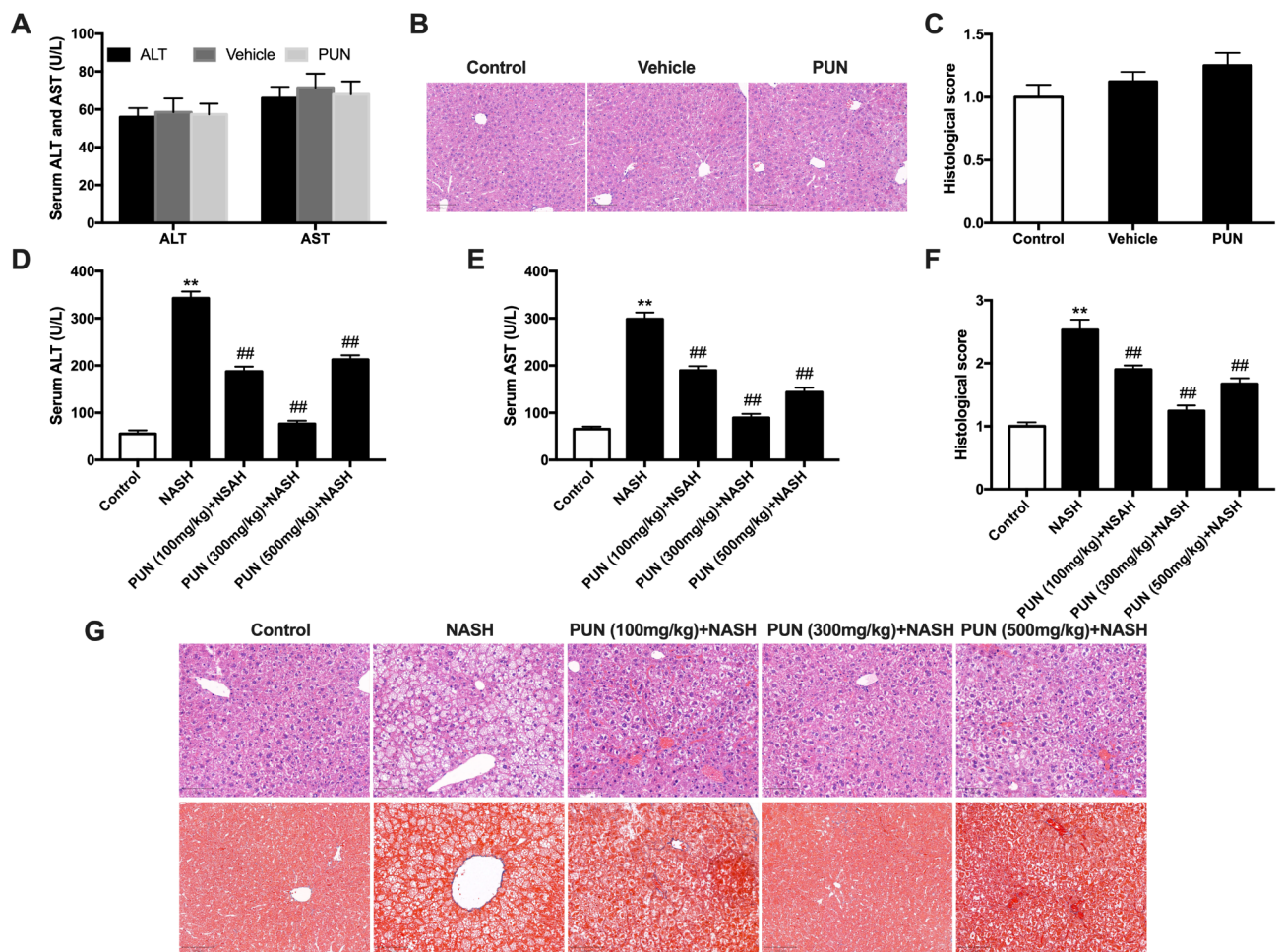


Fig. 1. PUN alleviated liver injury in diet-induced NASH. (A) Serum ALT and AST levels and liver hydroxyproline concentrations. Data are presented as the mean \pm SD ($n = 10$, from three independent experiments). (B, C) The H&E staining of liver tissues in the Control, vehicle and PUN (100, 300, 500 mg/kg) groups (original magnification, 200 \times). (D–E) Detection of ALT and AST concentrations in serum of PUN-treated mice after NASH. (F, G) H&E and Masson staining of liver tissues (original magnification, 200 \times). Similar results were obtained from three independent experiments. All data are presented as the mean \pm SEM ($n = 6$ in each group). * $P < 0.05$ and ** $P < 0.01$ vs. Control group; ## $P < 0.01$ vs. NASH group.

PUN attenuated the hepatic inflammatory response in diet-induced NASH

The number of infiltrating neutrophils was higher in the liver tissue of the NASH group compared to the control group. As shown in Fig. 2A–C, NASH stimulated serum levels of IL-1 β , IL-6 and TNF- α compared to the control group, whereas PUN relieved the production of inflammatory cytokines. Previous reports revealed that NASH-activated inflammation reaction is regulated by Txnip-NLRP3 inflammasome activation, which is interrelated to the occurrence and development of liver injury¹⁹. Interestingly, the results of Western blotting showed that the protein levels of Txnip, NLRP3, apoptosis-associated speck-like protein containing a CARD (ASC), Cleaved-Caspase1 and Mature-IL-1 β in the NASH group were significantly higher compared with the control group. However, PUN significantly lessened the protein abundance of Txnip, NLRP3, ASC, Cleaved-Caspase1 and IL-1 β (Fig. 2D–I), implying that inflammation inhibited by PUN may also be partly responsible for suppressing activation of the Txnip-NLRP3 inflammasome.

PUN enhanced antioxidant activity in diet-induced NASH

The results showed that liver superoxide dismutase (SOD) and glutathione peroxidase (GSH) activities were lower in the NASH group, and liver malondialdehyde (MDA) levels was increased compared with the control group. Mice that received PUN (100, 300, and 500 mg/kg i.g.) had higher activities of SOD and GSH, but simultaneously lower levels of liver MDA (Fig. 3A–C) compared with the NASH group. Mice treated with PUN had lower 2',7'-dichlorofluorescein-diacetate (DCFH-DA) fluorescence in liver tissue compared with the NASH group (Fig. 3D–E).

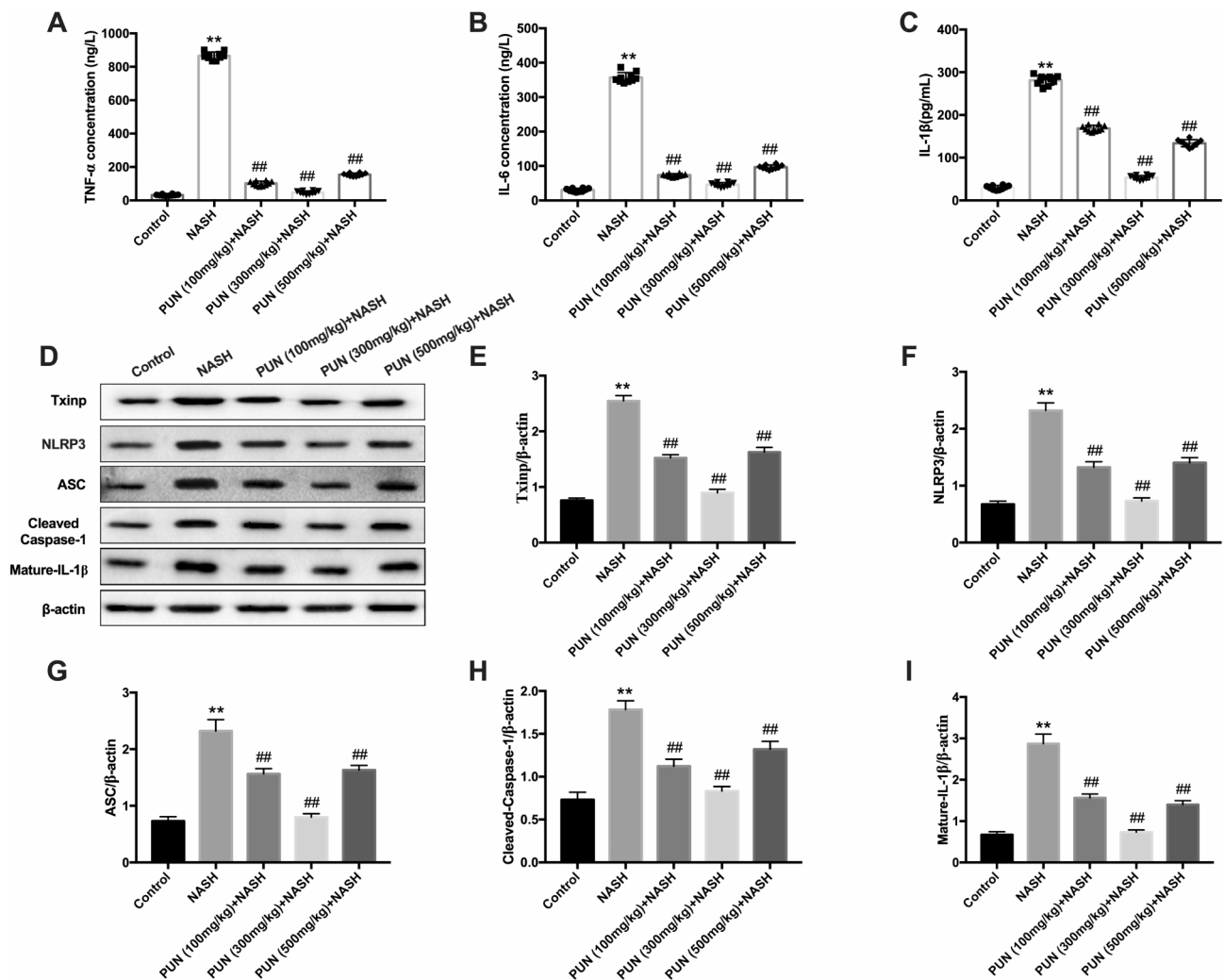


Fig. 2. PUN attenuated hepatic inflammatory response in mice with NASH. (A–C) Effects of PUN on NASH-induced serum TNF- α , IL-6, and IL-1 β generation. Similar results were obtained from three independent experiments. (D–G) Effects of PUN on NLRP3, ASC, cleaved-caspase-1, and mature-IL-1 β protein expression was measured by western blotting and quantification of protein expression was performed by densitometric analysis. Similar results were obtained from three independent experiments. All data are presented as the mean \pm SEM ($n=6$ in each group). * $p<0.05$ and ** $p<0.01$ vs. Control group; ## $p<0.01$ vs. NASH group.

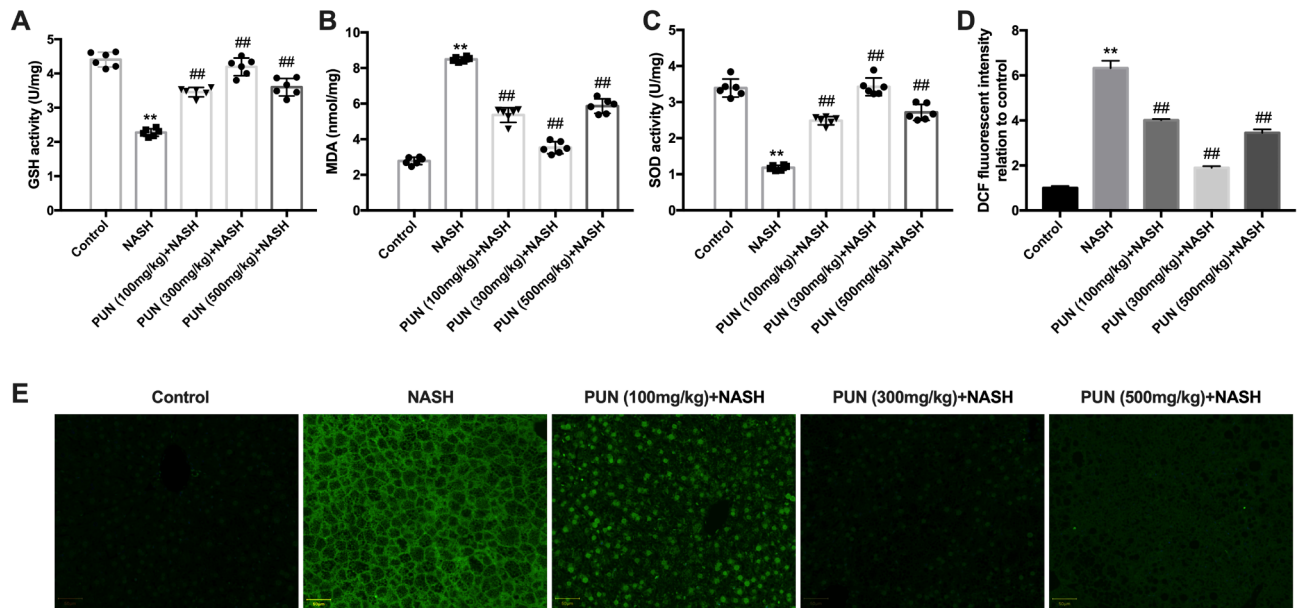


Fig. 3. PUN enhanced the antioxidant activities in the liver injury model induced by NASH. (A–C) The hepatic concentration of GSH, MDA and hepatic SOD activity after CDAH-induced NASH with or without intragastric infusion of PUN. (D–E) Cellular ROS estimated using the probe DCFH-DA by fluorescence microscopy. All data are presented as means \pm SEM ($n = 6$ in each group). * $P < 0.05$ and ** $P < 0.01$ vs. the NASH group.

PUN upregulated p62/Nrf-2 signaling in diet-induced NASH

The results showed that the expression of Nrf2 and p-p62 in cell nuclei were higher after treatment with PUN compared with control group (Fig. 4A–C). PUN treatment facilitated the expression of HO-1 and nuclear abundance of Nrf2 when compared with the NASH group (Fig. 4D–G). In addition, compared with NASH group, PUN treatment dramatically promoted phosphorylation of p62 at Ser349 in NASH mice (Fig. 4D–G). We speculate that PUN mediates the p62/Nrf2 signaling pathway to play a protective role in NASH-induced liver injury.

PUN up-regulated autophagy via the AMPK/mTOR/ULK1 signaling pathway

Considering that NASH can enhance autophagy and regulate oxidative stress, and plays an important role in improving NASH-induced hepatotoxicity, we measured the protein expression level of autophagy genes (including Beclin-1, LC3, Atg5 and Atg7). Compared with the NASH group, the protein expression of other autophagy genes decreased, and the protein expression was significantly restored by PUN treatment (Fig. 5A–E).

To study further how PUN regulated autophagy of NASH-induced liver injury, we examined the expression of p-AMPK, mTOR and p-ULK1 proteins. Compared with the control group, the expression of mTOR in the NASH group was significantly higher ($P < 0.05$), while the expression of p-AMPK and p-ULK1 in the NASH group was significantly lower ($P < 0.05$). PUN attenuated expression of p-AMPK, p-ULK1 and enhanced expression of mTOR, which was conducive to activation of autophagy (Fig. 5F–I). These results indicate that PUN may upregulate hepatocyte autophagy by inhibiting mTOR and upregulating expression phosphorylation of AMPK and ULK1.

PUN improved liver injury caused by NASH dependent upon Nrf2

The results showed that PUN-mediated reversion of serum ALT and AST in WT mice with NASH was significantly impeded in Nrf2^{-/-} mice (Fig. 6A, B). Administration of PUN (300 mg/kg) significantly suppressed the generation of ROS, TNF- α , IL-6 and IL-1 β in WT NASH mice, and these effects were blocked in Nrf2^{-/-} NASH mice (Fig. 6C–F). PUN relieved the histological changes in the liver of NASH mice, whereas the hepatoprotective role of PUN were interdicted in Nrf2^{-/-} mice of NASH, as determined by histological examination (Fig. 6G, H). More importantly, PUN (300 mg/kg) significantly suppressed the generation of Txinp, NLRP3, ASC, Cleaved-Caspase1 and Mature-IL-1 β in WT NASH mice, and these effects were blocked in Nrf2^{-/-} NASH mice (Fig. 7).

In addition, PUN up-regulated the concentrations of p62, Nrf2, HO-1, p-AMPK, p-ULK1, Beclin-1, LC3, Atg5 and Atg7 proteins, but down-regulated the abundance of p-mTOR in WT NASH mice. However, these effects were significantly weakened in Nrf2^{-/-} mice (Fig. 8).

Discussion

Overnutrition can lead to insulin resistance, diabetes, obesity and NAFLD²⁰. Non-alcoholic fatty liver disease covers a series of liver diseases, including steatosis, NASH and cirrhosis histologically². Hepatocyte inflammation, oxidative damage and fibrosis in NASH may eventually evolve into cancer³. Pomegranate and PUN are related

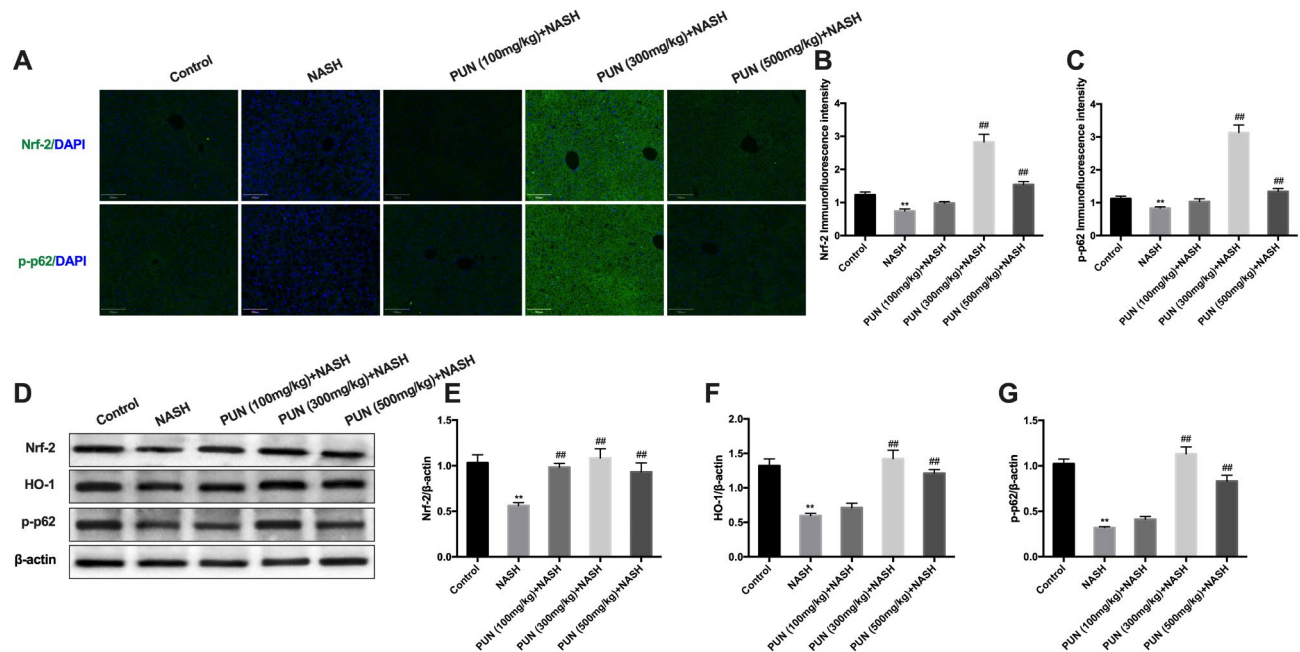


Fig. 4. PUN upregulated the p62/Nrf-2 signaling in mice with NASH-induced liver injury. (A–C) Immunofluorescence stained analysis of Nrf2 and p-p62 in liver tissues (original magnification, 200×). (D–G) Liver tissue was analyzed by western blot for assessment of nuclear abundance of Nrf2, HO-1 and phosphorylation of p62 at ser349. β-actin was used as an internal control. Similar results were obtained from three independent experiments. All data are presented as means ± SEM ($n = 6$ in each group). * $P < 0.05$ and ** $P < 0.01$ vs. Control group; # $P < 0.05$ and ## $P < 0.01$ vs. NASH group.

to various biological activities including antiobesity, antioxidative and anti-inflammatory effects^{21–23}. However, the pathogenic effects of PUN on diet-induced NASH are still unclear. In the present study, the effect and mechanism of PUN on oxidative stress and inflammation caused by diet-induced NASH were studied *in vivo*. The results indicated that PUN reduced hepatic steatosis, lymphocyte infiltration and hepatocyte hypertrophy in NASH mice, which may be a protective factor against hepatic steatosis. These results are closely related to the loss of Nrf2.

Liver inflammation has emerged as one of the important pathogenesis of NASH²⁴. In particular, the interaction between hepatocytes and fat cells is a key pathogenic factor^{25,26}. In the case of chronic obesity, more inflammatory cytokines including TNF-α, IL-1β and IL-6 are produced in liver tissue to initiate the inflammatory response. In the present study, treatment with PUN reduced neutrophil infiltration in the liver, and the concentration of TNF-α, IL-1β and IL-6 and other inflammatory markers in NASH. Similar to our findings, PUN can inhibit the secretion of proinflammatory cytokines induced by CCl₄ and downregulate the expression of TNF-α and IL-6 in hepatocytes of obese mice²⁶. Furthermore, the activation of inflammation and ROS generated also serves as a danger signal that activates NLRP3²⁷. Once NLRP3 is activated, the recruitment of ASC begins, followed by activation of caspase-1, and the maturation of inflammatory cytokines IL-1β, which is associated with the pathogenesis of liver injury²⁸. Our results indicated that PUN dramatically inhibited NASH-induced NLRP3, ASC, cleave-caspase-1, and mature-IL-1β protein expression. This shows that activation of the NLRP3 inflammasome was caused by a NASH-induced inflammatory response through Txnip-NLRP3 interaction.

As shown in previous studies, a HFD increases ROS and MDA in the liver, resulting in significant oxidative stress^{29,30}. We showed that PUN reduced ROS production and increased SOD and GSH, which further inhibited the oxidative stress response caused by NASH. PUN has strong antioxidant activity, accounting for more than 50% of the total antioxidant capacity of pomegranate³¹. PUN enhances the intracellular antioxidant response by up-regulating the expression of the antioxidant enzyme GSH. This increased antioxidant response is thought to be related to the Nrf2/HO-1 signaling, a defense mechanism against oxidative stress and cytotoxicity³². In the basal state, the transcription factor Nrf2 usually exists in the cytoplasm as a complex with HO-1, but when the cell is sensitive to ROS or electrophiles, Nrf2 is released from the complex into the nucleus, thereby promoting expression of antioxidants or antioxidant GSH metabolic enzymes³³. Therefore, PUN-mediated activation of Nrf2 signaling is believed to contribute to upregulation of endogenous antioxidants and reduce NASH-induced liver oxidative stress damage.

It is well known that activation of Nrf2 induces expression of p62/SQSTM1, and p62/SQSTM1 is the most studied member of the autophagy process. It is a multifunctional protein that can serve as a scaffold for signal transduction protein complexes and protein transport, Aggregation and degradation of the adaptor³⁴. p62/SQSTM1 also plays an important role in regulating the Nrf2 pathway. Nrf2 activation is associated with phosphorylation of p62 via competitive disruption of Nrf2 binding³⁵. In this study, we also examined the effect of PUN on p62 phosphorylation. We showed that PUN effectively induced Nrf2 translocation in mice with liver

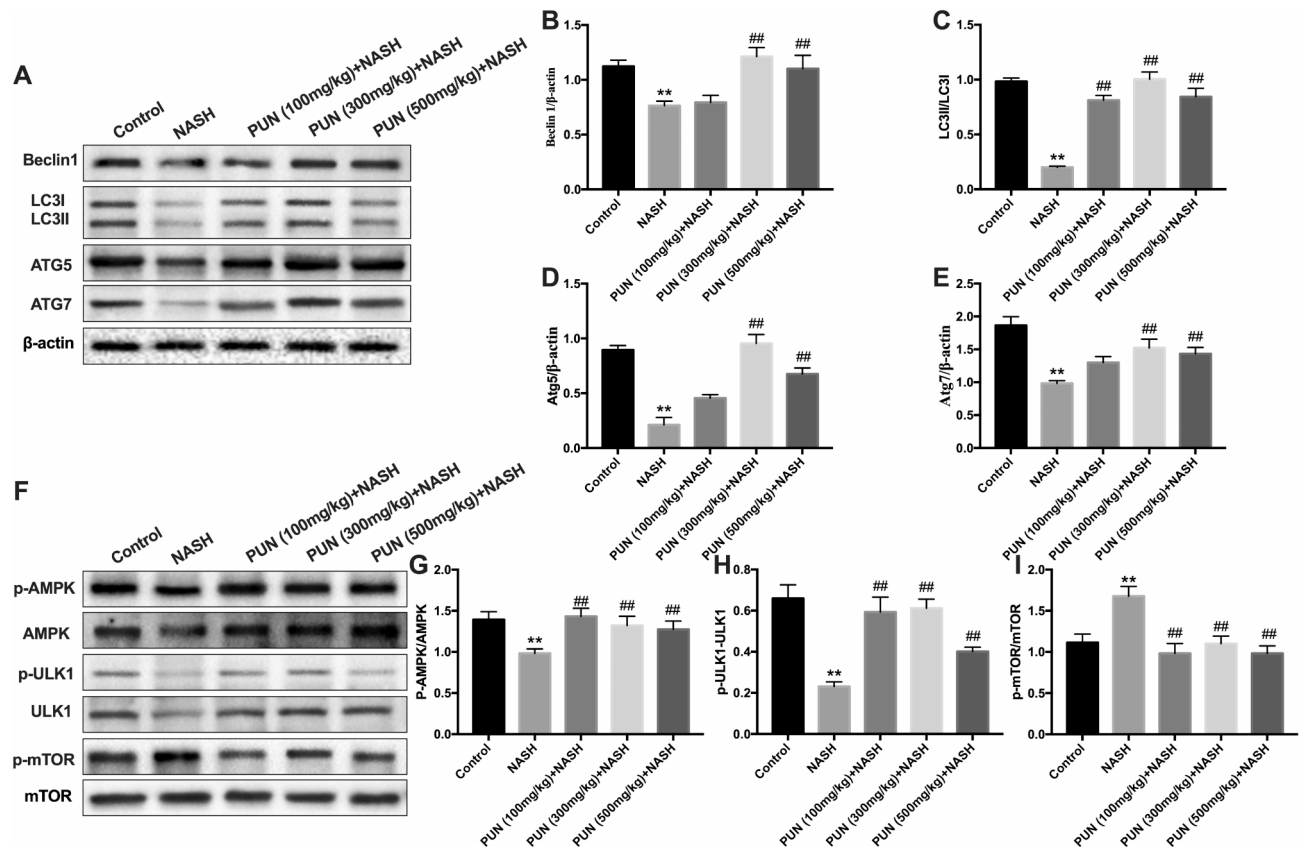


Fig. 5. PUN regulates up-regulated autophagy via the AMPK/mTOR/ULK1 signaling pathway. (A–E) Effects of PUN on protein abundance of Beclin-1, LC3, Atg5 and Atg7 measured by western blotting. (F–I) Effects of PUN on protein abundance of p-AMPK, p-mTOR and p-ULK1 measured by western blotting. Similar results were obtained from three independent experiments. All data are presented as means \pm SEM ($n = 6$ in each group). * $P < 0.05$ and ** $P < 0.01$ vs. Control group; # $P < 0.05$ and ## $P < 0.01$ vs. NASH group.

injury in NASH, p62 phosphorylation at Ser349, and HO-1 abundance. These results indicate that Nrf2 may play an important role in preventing liver damage induced by NASH.

There is increasing evidence that induction of autophagy can reduce the occurrence of various liver diseases by regulating activation of inflammation and oxidative stress, which indicates that autophagy plays a key role in improving liver toxicity caused by NASH. Sustained autophagy can reduce NASH-induced liver damage by regulating oxidative properties³⁶. In our study, PUN induced autophagy by upregulating the abundance of Atg5, Atg7, Beclin-1 and LC3 proteins; however, all of these were reduced by NASH-induced liver damage. The transcription factor mTOR plays a crucial role in the control of autophagy, and its function is partially regulated by the AMPK/mTOR/ULK1 signaling pathway. In our study, PUN enhanced the phosphorylation of AMPK and ULK1, and inhibited induction of mTOR in NASH-induced liver injury. These responses indicate that PUN-induced autophagy activation may depend on the AMPK/mTOR/ULK1 signaling pathway.

Knockdown of Nrf2 prevented PUN-mediated inhibition of the expression of inflammatory cytokines and oxidative stress indicators, indicating that PUN-mediated inhibition of NASH-induced inflammation and oxidative stress depends on the Nrf2 signaling pathway. It is worth noting that, in our study, compared with WT mice, NASH caused a decrease in the abundance of autophagy proteins in Nrf2^{-/-} mice, while PUN treatment increased the abundance of autophagy proteins. These results indicate that Nrf2 deficiency leads to upregulation of autophagy, which may clarify the hepatoprotective effect observed with PUN in Nrf2^{-/-} mice.

In this study, PUN demonstrated a non-linear, U-shaped dose-response relationship. The 300 mg/kg dose exhibited the most significant therapeutic effect, outperforming both the 100 mg/kg and 500 mg/kg doses, although the latter also showed some benefit. This phenomenon may be linked to a biological optimization mechanism. We hypothesize that at the lower 100 mg/kg dose, PUN may be insufficient to trigger a full therapeutic effect, while at the higher 500 mg/kg dose, despite its antioxidant properties and autophagy enhancement, the excessive dose may induce physiological suppression or side effects, limiting further therapeutic improvement. This non-dose-dependent response may reflect the body's drive toward biological optimization, where an optimal therapeutic dose exists, and exceeding this dose may reduce effectiveness. The U-shaped dose-response relationship also represents a limitation of our study. Although the 300 mg/kg dose produced the best therapeutic outcome, the absence of a clear, linear dose-response relationship complicates the establishment of precise therapeutic guidelines. The potential adverse effects observed at the higher 500 mg/kg dose highlight the need for further

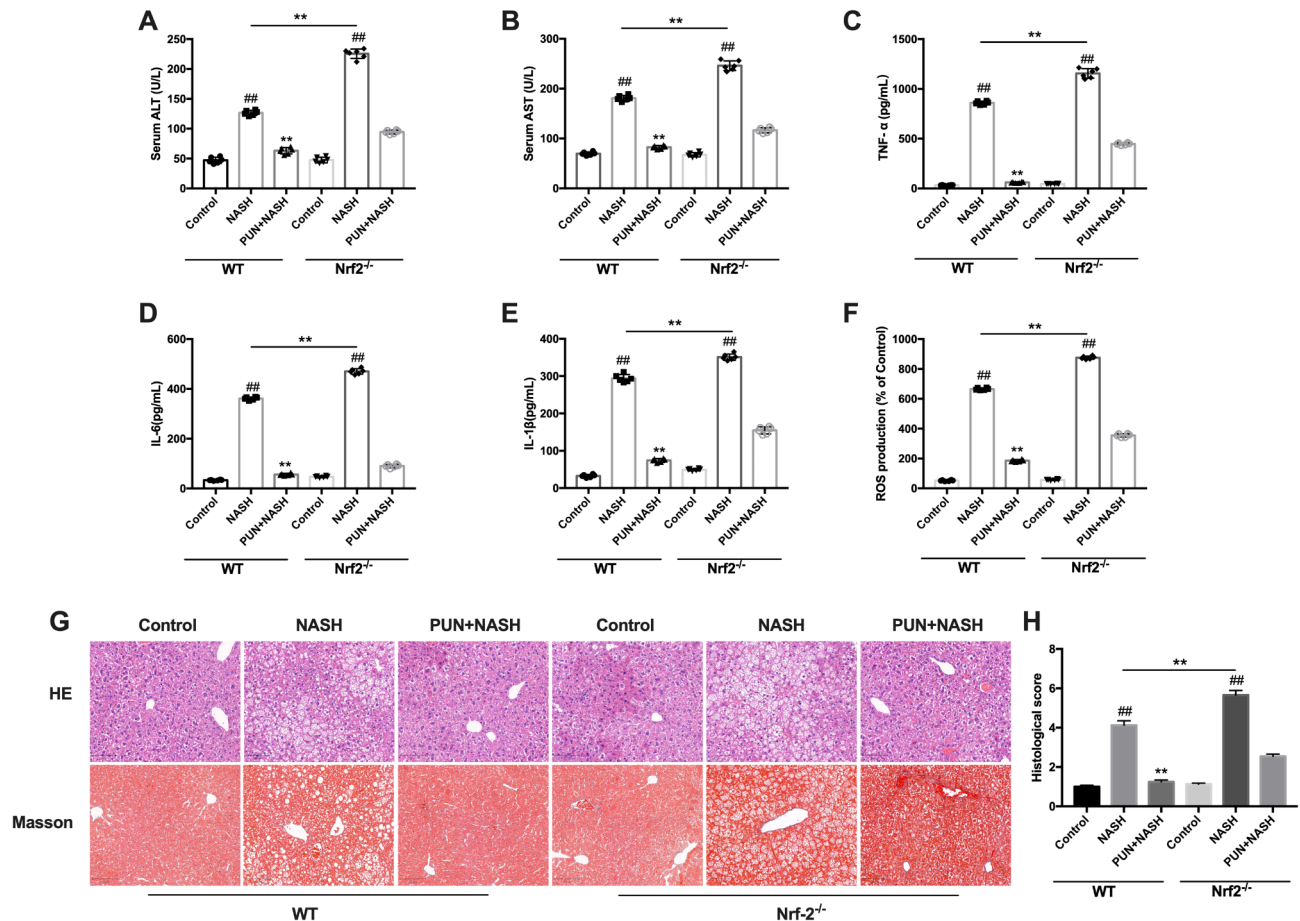


Fig. 6. PUN improved liver injury caused by NASH dependent upon Nrf2 deficiency in mice. WT and Nrf2^{-/-} mice were injected intraperitoneally with PUN (300 mg/kg) for 24 h followed by challenge with NASH. (A–B) Blood serum collected assessment of ALT and AST activities. (C–F) Liver tissues serum TNF-α, IL-6, and IL-1β and ROS generation. Similar results were obtained from three independent experiments. (G, H) Representative histological sections of liver were stained with H&E and Masson (magnification×400). Similar results were obtained from three independent experiments. All data are presented as means ± SEM (*n* = 6 in each group). **P* < 0.05 and ***P* < 0.01 vs. Control group; #*P* < 0.05 and ##*P* < 0.01 vs. NASH group.

research into the underlying mechanisms, as well as the safety and efficacy of different doses. Additionally, the study did not explore a broader range of doses or temporal factors, limiting a comprehensive understanding of the pharmacokinetics and long-term effects of PUN. Future studies are essential to clarify the optimal dosing regimen, explore the involved biological mechanisms, and optimize dosage for clinical applications.

In summary, we showed that PUN plays a role in protecting against liver injury through possible mechanisms involved in Nrf2 activation and induction of autophagy. We found that compared with WT mice, NASH reduced activation of the autophagy proteins Atg7, Atg5, Beclin-1 and LC3 in Nrf2^{-/-} mice, and PUN restored autophagy protein expression levels. Overall, this study provides new insights into the mechanism by which PUN protects the liver from inflammation, oxidative stress and autophagy during NASH-induced liver injury (Fig. 9).

Materials and methods

Reagents

Punicalagin was purchased from Sigma-Aldrich (cat. no. P0023; St. Louis, MO, USA). Dimethyl sulfoxide obtained from Sigma-Aldrich. Antibodies against Nrf2, SQSTM1/p62 (phospho S349), p-ULK1, p-mTOR and p-AMPK were obtained from Abcam (Cambridge, UK); HO-1, Beclin1, LC3, Atg5, Atg7, NLRP3, ASC, Cleaved Caspase1, IL-1β, ULK1, mTOR and AMPK and β-actin were obtained from Proteintech; Test kits of malondialdehyde (MDA), reactive oxygen species (ROS), GSH, and superoxide dismutase (SOD), alanine transaminase (ALT), aspartate aminotransferase (AST) were obtained from Nanjing Jiancheng Bioengineering Institute (Nanjing, China).

Animals

Wild-type (WT) and Nrf2 KO (Nrf2^{-/-}) C57BL/6 male mice (18–22 g, 6–8 weeks old) were purchased from Cyagen Biosciences (Guangzhou, China; Certificate No. KOAIP190930WZ1). All animals were maintained

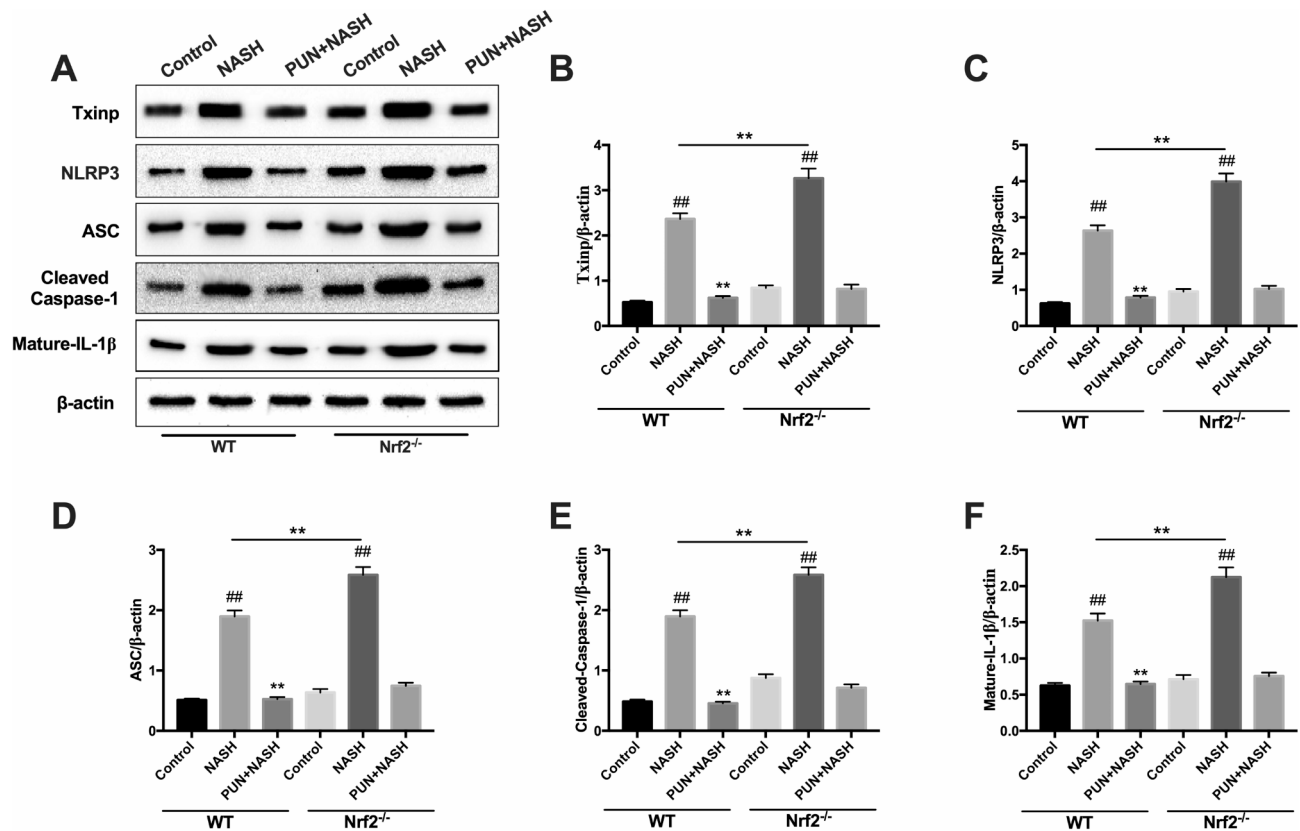


Fig. 7. PUN improved Txnip-NLRP3 signaling pathway caused by NASH dependent upon Nrf2 deficiency in mice. WT and Nrf2 $^{-/-}$ mice were injected intraperitoneally with PUN (300 mg/kg) for 24 h followed by challenge with NASH. (A–F) Effects of PUN on protein abundance of Txnip, NLRP3, ASC, Cleaved-Caspase1 and Mature-IL-1 β measured by western blot. β -actin was used as an internal control. Similar results were obtained from three independent experiments. All data are presented as means \pm SEM ($n = 6$ in each group). * P < 0.05 and ** P < 0.01 vs. Control group; # P < 0.05 and ## P < 0.01 vs. NASH group.

under standard SPF conditions with 50~60% humidity and a 12:12 light: dark cycle and with free access to sterile water and food. The Animal Ethics Committee of Heilongjiang Bayi Agricultural University (Daqing, China) approved the study protocol. All animal experimental procedures were conducted in accordance with China's Public Health Service Policy and were approved by the Guidelines for the Care and Use of Experimental Animals in Heilongjiang Bayi Agricultural University (Approval No: DWKJXY2023019). The procedures fully complied with the approved guidelines and the ARRIVE guidelines (<https://arriveguidelines.org>).

Diets and experimental design

The mouse model of diet-induced NASH was established by feeding a choline-deficient, L-amino acid-defined, high-fat (CDAAH) diet (60 kcal% fat) obtained from Research Diets (cas no. A06071302; NJ, USA) for 12 weeks³⁷. The control group was fed with a pellet chow diet consisting of 10 kcal% fat (D12450J; Research Diets, New Brunswick, NJ, USA). Mice were fed the HFD diet induced NASH and treated with PUN by gavage for 12 weeks. To assess the protective effect of PUN against NASH, WT mice were randomly divided into five groups ($n = 10$): Control (vehicle-treated) group, NASH group, and PUN (dissolved in saline; 100, 300 or 500 mg/kg bw/day, i.g.)-treated + NASH group.

To explore the participation of Nrf2 in the hepatoprotective effects of PUN against diet-induced NASH, WT or Nrf2 $^{-/-}$ mice were divided into three groups ($n = 6$ mice): Control (vehicle-treated) group, NASH group, PUN (300 mg/kg bw/day, i.g.)-treated + NASH group.

All mice were euthanized 24 h after the final treatment, anesthetized intraperitoneally with pentobarbital (70 mg/kg bw), and then subjected to cervical dislocation. Serum and liver tissue were collected at the time of sacrifice for biochemical assays, ELISA or Western blot analysis, and histopathological examination.

Histopathological/Masson staining

Formalin-fixed, paraffin-embedded sections of liver tissue were cut into 5 μ m thick and stained with hematoxylin-eosin or Masson's trichrome to evaluate hepatic pathological changes using light microscopy.

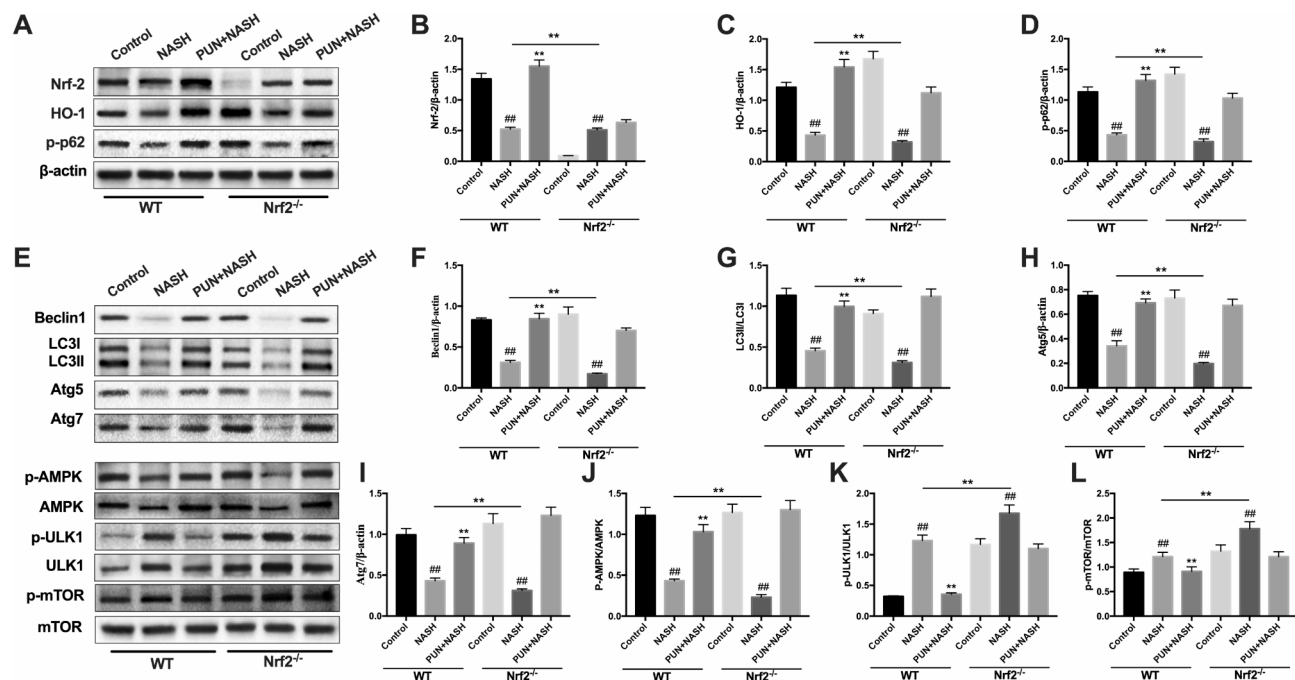


Fig. 8. PUN improved Autophagy caused by NASH dependent upon Nrf2 deficiency in mice. WT and Nrf2^{-/-} mice were injected intraperitoneally with PUN (300 mg/kg) for 24 h followed by challenge with NASH. (A–E) Effects of PUN on protein abundance of Beclin-1, Atg5, Atg7, LC3, p-AMPK, p-ULK1 and p-mTOR measured by western blot. β-actin was used as an internal control. Similar results were obtained from three independent experiments. All data are presented as means ± SEM (*n* = 6 in each group). **P* < 0.05 and ***P* < 0.01 vs. Control group; #*P* < 0.05 and ##*P* < 0.01 vs. NASH group.

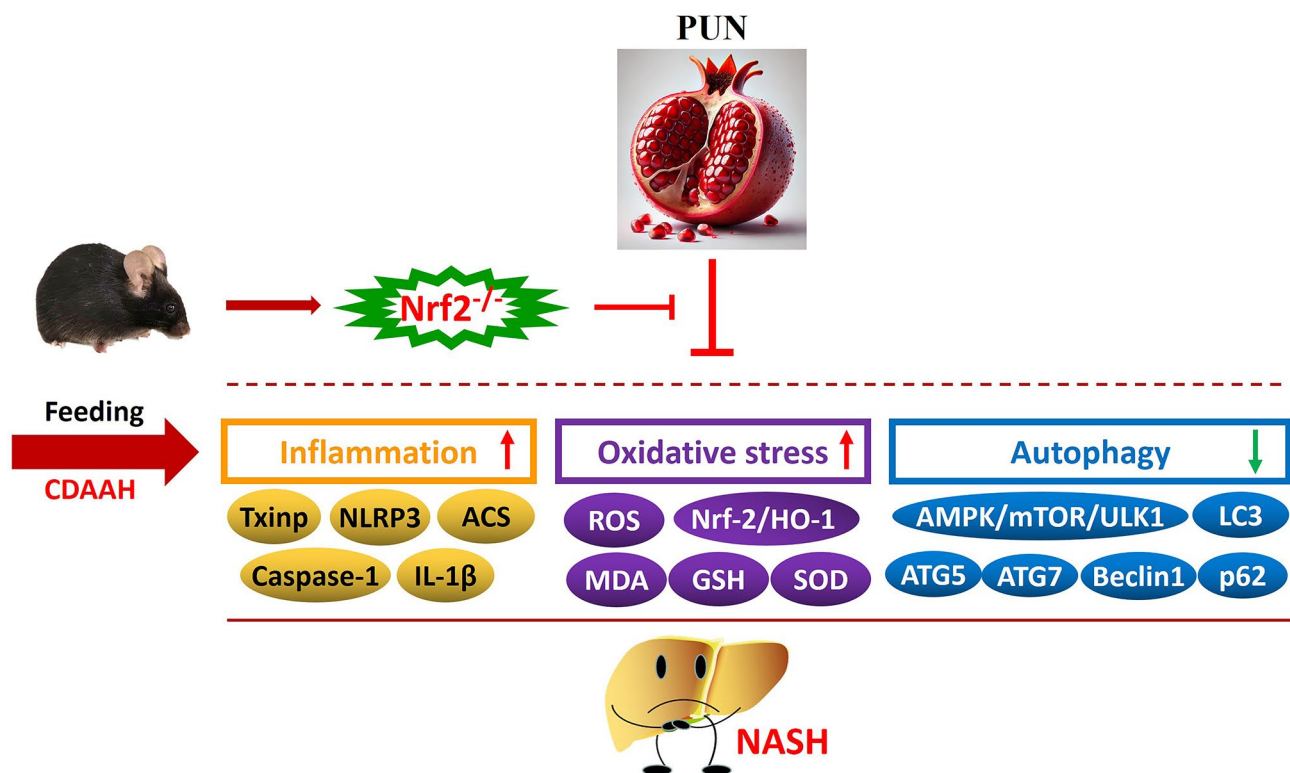


Fig. 9. Punicalagin Relieves Hepatic Injury by Antioxidation and Enhancement of Autophagy in diet-induced Nonalcoholic Steatohepatitis.

Immunofluorescence

Frozen liver samples were fixed in paraformaldehyde (4%) for 30 min and washed with PBS. Slides were blocked with 3% BSA for 2 h, and then incubated with primary Nrf2 and p-p62 antibody at 4 °C overnight. These sections were subsequently washed and treated with Alexa Fluor Plus 488 goat anti-rabbit IgG secondary antibody for 1 h. Additionally, the nuclei were stained with DAPI. Fluorescent changes were examined under a confocal microscope.

Measurement of liver function index and oxidative stress

The concentration of ALT and AST in serum and liver were detected using commercially obtained kits according to the manufacturer's instructions. Liver tissue was homogenized in extraction buffer to analyze the ROS, MDA, GSH and SOD levels in accordance with the manufacturer's instructions. The data were normalized in terms of total protein concentration in each sample.

Enzyme-linked immunosorbent assay (ELISA)

Inflammation biomarkers including TNF- α , IL-6, and IL-1 β in blood serum was performed using ELISA kits following the manufacturer's instructions (BioLegend, San Diego, CA, USA) and the absorbance were read at 450 nm.

Reactive oxygen species (ROS) production assay

Reactive oxygen species generation was assayed using DCFH-DA fluorescent probes (cas no. D6470; Solarbio, China). Hepatocyte suspensions derived from liver samples were incubated with 10 μ M DCFH-DA for 1 h at 37 °C. The medium was subsequently discarded and cells were washed with PBS solution. The ROS generation was evaluated by a fluorescence spectrometry, and images were obtained with a fluorescence microscope (Olympus, Japan).

Western blot analysis

Western blot analysis was performed as previously reported³⁷. Briefly, total proteins from each sample were separated by a 12% SDS-PAGE and transferred onto 0.45 μ m PVDF membrane. The membranes were blocked with 5% (w/v) nonfat milk for 2 h. The blocked membranes were incubated with primary antibodies (NLRP3, ASC, Cleaved Caspase1, IL-1 β , Nrf2, HO-1, p-AMPK, AMPK, Atg5, Atg7, p-p62, p-mTOR, mTOR, p-ULK1, ULK1, Beclin1, LC3 and β -actin) and secondary antibody (anti-rabbit IgG and anti-mouse IgG). Lastly, the membranes were visualized using ECL western blotting detection reagent in western blotting analysis system with Image Lab (Bio-Rad, PA, USA).

Statistical analysis

All data were analyzed using the SPSS software version 25.0 (IBM, Chicago, IL, USA) and expressed as the mean \pm SEM. One-way ANOVA was performed for multiple comparisons with Bonferroni correction. A *P*-value < 0.05 was considered statistically significant and a *P*-value < 0.01 was considered highly significant.

Data availability

All data generated or analysed during this study are included in this article.

Received: 23 January 2025; Accepted: 9 April 2025

Published online: 25 April 2025

References

1. Younossi, Z. M. et al. Global epidemiology of nonalcoholic fatty liver disease-Meta-analytic assessment of prevalence, incidence, and outcomes. *J. Hepatol.* **64**, 73–84. <https://doi.org/10.1002/hep.28431> (2016).
2. Ibrahim, S. H., Hirsova, P. & Gores, G. J. Non-alcoholic steatohepatitis patho-genesis: Sublethal hepatocyte injury as a driver of liver inflammation. *J. Gut.* **67**, 963–972. <https://doi.org/10.1136/gutjnl-2017-315691> (2018).
3. Fingas, C. D. et al. Epidemiology of non-alcoholic steatohepatitis and hepatocellular carcinoma. *J. Clin. Liver Dis.* **8**, 119–122. <https://doi.org/10.1002/cld.585> (2016).
4. Surh, Y. J., Kundu, J. K. & Na, H. K. Nrf2 as a master redox switch in turning on the cellular signaling involved in the induction of cytoprotective genes by some chemopreventive phytochemicals. *J. Planta Me.* **74**, 1526–1539. <https://doi.org/10.1055/s-0028-1088302> (2008).
5. Zhu, H. et al. Nrf2 controls bone marrow stromal cell susceptibility to oxidative and electrophilic stress. *J. Free Radic Biol. Med.* **41**, 132–43. [https://doi.org/10.1016/j.freeradbiomed.2006.03.02\(2006\)](https://doi.org/10.1016/j.freeradbiomed.2006.03.02(2006)).
6. Jin, W. et al. Genetic ablation of Nrf2 enhances susceptibility to acute lung injury after traumatic brain injury in mice. *J. Exp. Biol. Med.* **2**, 181–189. [https://doi.org/10.1016/S0094-5765\(98\)00034-4](https://doi.org/10.1016/S0094-5765(98)00034-4) (2009).
7. Osburn, W. O. et al. Nrf2 regulates an adaptive response protecting against oxidative damage following diquat-mediated formation of superoxide anion. *J. Arch. Biochem. Biophys.* **454**, 7–15. [https://doi.org/10.1016/j.abb.2006.08.005\(2006\)](https://doi.org/10.1016/j.abb.2006.08.005(2006)).
8. Lv, H. et al. Asiatic acid exhibits Anti-inflammatory and antioxidant activities against lipopolysaccharide and d-Galactosamine-Induced fulminant hepatic failure. *J. Front. Immunol.* **8**, 785. <https://doi.org/10.3389/fimmu.2017.00785> (2017).
9. Jia, Y. N. et al. Oxyresveratrol prevents lipopolysaccharide/ d-galactosamine-induced acute liver injury in mice. *J. Int. Immunopharmacol.* **56**, 105–112. [https://doi.org/10.1016/j.intimp.2018.01.014\(2018\)](https://doi.org/10.1016/j.intimp.2018.01.014(2018)).
10. Swanson, M. S. & Molofsky, A. B. Autophagy and inflammatory cell death, partners of innate immunity. *J. Autophag.* **3**, 174–176. [https://doi.org/10.4161/auto.1.3.2067\(2005\)](https://doi.org/10.4161/auto.1.3.2067(2005)).
11. Scherz-Shouval, R. et al. Reactive oxygen species are essential for autophagy and specifically regulate the activity of Atg4. *J. EMBO.* **7**, 1749–1760. <https://doi.org/10.1038/sj.emboj.7601623> (2007).
12. Zhou, X. et al. Artesunate induces autophagy dependent apoptosis through upregulating ROS and activating AMPK-mTOR-ULK1 axis in human bladder cancer cells. *J. Chem. Biol. Interact.* **331**, 109273. <https://doi.org/10.1016/j.cbi.2020.109273> (2020).

13. Lavallard, V. Autophagy and non-alcoholic fatty liver disease. *J. Biomed. Biotechnol.* **4**, 120179. <https://doi.org/10.1155/2014/120179> (2014).
14. Lyu, A. et al. Punicalagin protects bovine endometrial epithelial cells against lipopolysaccharide-induced inflammatory injury. *J. Zhejiang Univ. Sci. B.* **6**, 481–491. <https://doi.org/10.1631/jzus.b1600224> (2017).
15. Mo, F. F. et al. Protective mechanism of punicalagin against endoplasmic reticulum stress in the liver of mice with type 2 diabetes mellitus. *J. Funct. Foods* **56**, 57–64. <https://doi.org/10.1016/j.jff.2019.03.006> (2019).
16. Yu, L. M. et al. Protection of the myocardium against ischemia/reperfusion injury by Punicalagin through an SIRT1-NRF-2-HO-1-dependent mechanism. *J. Chem. Biol. Interact.* **306**, 152–162. <https://doi.org/10.1016/j.cbi.2019.05.003> (2019).
17. Liu, H. et al. Punicalagin prevents hepatic steatosis through improving lipid homeostasis and inflammation in liver and adipose tissue and modulating gut microbiota in Western Diet-Fed mice. *Mol. Nutr. Food Res.* **65** (4), e2001031. <https://doi.org/10.1002/mnfr.202001031> (2021).
18. Tan, X. et al. Punicalagin ameliorates diabetic liver injury by inhibiting pyroptosis and promoting autophagy via modulation of the FoxO1/TXNIP signaling pathway. *Mol. Nutr. Food Res.* **68** (12), e2300912. <https://doi.org/10.1002/mnfr.202300912> (2024).
19. Mridha, A. R. et al. NLRP3 inflammasome Blockade reduces liver inflammation and fibrosis in experimental NASH in mice. *J. Hepatol.* **66**(5):1037–1046. <https://doi.org/10.1016/j.jhep.2017.01.022> (2017).
20. Meli, R. et al. High fat diet induces liver steatosis and early dysregulation of iron metabolism in rats. *J. PLoS One.* **6**, e66570. <https://doi.org/10.1371/journal.pone.0066570> (2013).
21. El-Beih, N. M. et al. Effects of pomegranate Aril juice and its Punicalagin on some key regulators of insulin resistance and oxidative liver injury in streptozotocin-nicotinamide type 2 diabetic rats. *J. Mol. Biol. Rep.* **4**, 3701–3711. <https://doi.org/10.1007/s11033-019-04813-8> (2019).
22. F. L. et al. Bioactive properties of commercialised pomegranate (*Punica granatum*) juice: Antioxidant, antiproliferative and enzyme inhibiting activities. *J. Food Funct.* **6**, 2049–2057. <https://doi.org/10.1039/c5fo00426h> (2015).
23. Pinheiro, A. J. M. C. R. et al. Leaf extract attenuates lung inflammation in mice with acute lung injury. *J. Immunol. Res.* **3**, 1–11. <https://doi.org/10.1155/2018/6879183> (2018).
24. Furukawa, S. et al. Increased oxidative stress in obesity and its impact on metabolic syndrome. *J. Clin. Invest.* **112**, 1752–1761. <https://doi.org/10.1172/JCI21625> (2004).
25. Lumeng, C. N., Bodzin, J. L. & Saltiel, A. R. Obesity induces a phenotypic switch in adipose tissue macrophage polarization. *J. Clin. Invest.* **117**, 175–184. <https://doi.org/10.1172/JCI29881> (2007).
26. Luo, J. et al. Punicalagin reversed the hepatic injury of tetrachloromethane by antioxidation and enhancement of autophagy. *J. Med. Food.* **12**, 1271–1279. <https://doi.org/10.1089/jmf.2019.4411> (2019).
27. Wan, X. et al. Role of NLRP3 inflammasome in the progression of NAFLD to NASH. *J. Can. J. Gastroenterol. Hepatol.* <https://doi.org/10.1155/2016/6489012> (2016).
28. Torres, S. et al. Mitochondria and the NLRP3 inflammasome in alcoholic and nonalcoholic steatohepatitis. *J. Cells.* **11**, 1475. <https://doi.org/10.3390/cells11091475> (2022).
29. Xu, Q., Fan, Y. & Loo, J. J. Aloin protects mice from diet-induced non-alcoholic steatohepatitis via activation of Nrf2/HO-1 signaling. *J. Food Funct.* **2**, 696–705. <https://doi.org/10.1039/D0FO02684K> (2021).
30. Ibrahim, S. H. et al. Non-alcoholic steatohepatitis pathogenesis: Sublethal hepatocyte injury as a driver of liver inflammation. *J. Gut.* **5**, 963–972. <https://doi.org/10.1136/gutjnl-315691> (2018).
31. Gil, M. I. et al. Antioxidant activity of pomegranate juice and its relationship with phenolic composition and processing. *J. Agric. Food Chem.* **48**, 4581–4589. <https://doi.org/10.1021/jf000404a> (2000).
32. Loboda, A. et al. Role of Nrf2/HO-1 system in development, oxidative stress response and diseases: An evolutionarily conserved mechanism. *J. Cell. Mol. Life Sci.* **73**, 3221–3247. <https://doi.org/10.1007/s00018-016-2223-0> (2016).
33. Lau, A. et al. A noncanonical mechanism of Nrf2 activation by autophagy deficiency: Direct interaction between Keap1 and p62. *J. Mol. Cell. Biol.* **13**, 3275–3285. <https://doi.org/10.1128/mcb.00248-10> (2010).
34. Komatsu, M. et al. The selective autophagy substrate p62 activates the stress responsive transcription factor Nrf2 through inactivation of Keap1. *J. Nat. Cell. Biol.* **3**, 213–223. <https://doi.org/10.1038/NCB2021> (2010).
35. Lavallard, V. J. & Gual, P. Autophagy and non-alcoholic fatty liver disease. *J. Biomed. Res. Int.* **4**, 120179. <https://doi.org/10.1155/2014/120179> (2014).
36. Matsumoto, M. et al. An improved mouse model that rapidly develops fibrosis in non-alcoholic steatohepatitis. *J. Int. J. Exp. Pathol.* **2**, 93–103. <https://doi.org/10.1111/iep.12008> (2008).
37. Xu, Q. et al. All-trans retinoic acid inhibits lipopolysaccharide-induced inflammatory responses in bovine adipocytes via TGFβ1/Smad3 signaling pathway. *J. BMC Vet. Res.* **1**, 48. <https://doi.org/10.1186/s12917-019-1791-2> (2019).

Author contributions

Data curation, ML; Formal analysis, XQS ; Funding acquisition, ML and XQS; Investigation, XN ; Methodology, SHB and XQS; Resources, ML; Software, ML and XQS ; Writing original draft, ML and XQS; Writing review&editing, ML and XQS.

Funding

This study was supported by grants from the Central Government Support for Local Universities Reform and Development Fund-Outstanding Young Talent Program, the Personnel Foundation in Heilongjiang Bayi Agricultural University (Daqing, China; Grant no. XYB202106), the National Natural Science Foundation of China (Grant. 32302834), Heilongjiang Bayi Agricultural University Postgraduate Innovative Research Project (Grant. YJSCX2023-Y24).

Declarations

Competing interests

The authors declare no competing interests.

Additional information

Supplementary Information The online version contains supplementary material available at <https://doi.org/10.1038/s41598-025-98044-6>.

Correspondence and requests for materials should be addressed to Q.X.

Reprints and permissions information is available at www.nature.com/reprints.

Publisher's note Springer Nature remains neutral with regard to jurisdictional claims in published maps and institutional affiliations.

Open Access This article is licensed under a Creative Commons Attribution-NonCommercial-NoDerivatives 4.0 International License, which permits any non-commercial use, sharing, distribution and reproduction in any medium or format, as long as you give appropriate credit to the original author(s) and the source, provide a link to the Creative Commons licence, and indicate if you modified the licensed material. You do not have permission under this licence to share adapted material derived from this article or parts of it. The images or other third party material in this article are included in the article's Creative Commons licence, unless indicated otherwise in a credit line to the material. If material is not included in the article's Creative Commons licence and your intended use is not permitted by statutory regulation or exceeds the permitted use, you will need to obtain permission directly from the copyright holder. To view a copy of this licence, visit <http://creativecommons.org/licenses/by-nc-nd/4.0/>.

© The Author(s) 2025